RED CELLS, IRON, AND ERYTHROPOIESIS

Abnormal properties of red blood cells suggest a role in the pathophysiology of Gaucher disease

Melanie Franco,[1-4] *Emmanuel Collec,[1-4] *Philippe Connes,[1,4,5] Emile van den Akker,[6] Thierry Billette de Villemeur,[7,8] Nadia Belmatoug,[8,9] Marieke von Lindern,[6] Nejma Ameziane,[1-4] Olivier Hermine,[4,10] Yves Colin,[1-4] *Caroline Le Van Kim,[1-4] and *Cyril Mignot[7,8]

[1]Inserm U665, Paris, France; [2]Université Paris Diderot, Sorbonne Paris Cité, UMR_S665, Paris, France; [3]Institut National de la Transfusion Sanguine, Paris, France; [4]Laboratoire d'excellence GR-Ex, Paris, France; [5]Université des Antilles et de la Guyane, Pointe-à-Pitre, Guadeloupe, France; [6]Sanquin Research and Landsteiner Laboratory, Academic Medical Center and Amsterdam University, Amsterdam, The Netherlands; [7]Service de Neuropédiatrie, Hôpital Trousseau, Assistance Publique–Hôpitaux de Paris and Université Pierre et Marie Curie, Paris, France; [8]Centre de Référence des Maladies Lysosomales, Clichy, France; [9]Service de Médecine Interne, Hôpital Beaujon, Clichy, France; and [10]CNRS UMR8147 and Service d'Hématologie, Hôpital Necker, Paris, France

Key Points

- We provide evidence that red blood cells from patients suffering from Gaucher diseases exhibit morphologic and functional abnormalities.

Gaucher disease (GD) is a lysosomal storage disorder caused by glucocerebrosidase deficiency. It is notably characterized by splenomegaly, complex skeletal involvement, ischemic events of the spleen and bones, and the accumulation of Gaucher cells in several organs. We hypothesized that red blood cells (RBCs) might be involved in some features of GD and studied the adhesive and hemorheologic properties of RBCs from GD patients. Hemorheologic analyses revealed enhanced blood viscosity, increased aggregation, and disaggregation threshold of GD RBCs compared with control (CTR) RBCs. GD RBCs also exhibited frequent morphologic abnormalities and lower deformability. Under physiologic flow conditions, GD RBCs adhered more strongly to human microvascular endothelial cells and to laminin than CTR. We showed that Lu/BCAM, the unique erythroid laminin receptor, is overexpressed and highly phosphorylated in GD RBCs, and may play a major role in the adhesion process. The demonstration that GD RBCs have abnormal rheologic and adhesion properties suggests that they may trigger ischemic events in GD, and possibly phagocytosis by macrophages, leading to the appearance of pathogenic Gaucher cells. (*Blood*. 2013;121(3):546-555)

Introduction

Gaucher disease (GD) is caused by β-glucocerebrosidase (GluCerase) deficiency and is the most common autosomal recessive lysosomal storage disorder. GD is a multisystem disorder with high clinical heterogeneity. Ten percent of GD patients, including fetuses (fetal GD), infants (type 2), older children, and adults (type 3), have signs of central nervous system involvement. However, the majority of patients belong to the subgroup of nonneuronopathic GD (type 1). In patients with GD1 and GD3, visceral enlargement (splenomegaly and hepatomegaly), hematologic manifestations (anemia, thrombocytopenia), and bone involvement are the most frequent and significant features of the condition.[1-3] Bone disease, a major characteristic of GD1,[4-7] is characterized by chronic features related to bone fragility (osteopenia/osteoporosis, osseous deformity, thinning of long bones cortex),[8,9] as well as acute or subacute events related to bone infarcts, such as bone infarcts ("bone crises") and avascular necrosis (AVN) of the head of long bones or of vertebral bodies. Ischemic events also occur in the spleen. The spleen of untreated patients may become large and fibrotic and contains numerous abnormal macrophages called Gaucher cells.

GluCerase deficiency results in the accumulation of its substrate, glucosylceramide (GlcCer), into macrophages because these cells are natural phagocytes that are involved in the degradation of membrane glycolipids from red blood cells (RBCs) and leukocytes. GlcCer-laden macrophages are not killed by the accumulation of the substrate, but tend to transform into Gaucher cells. Although dysfunction of macrophages/Gaucher cells is probably involved in the pathophysiology of many aspects of GD, other cell types could be involved as well.[2]In vitro studies and animal models showed that GluCerase deficiency reduces the differentiation of bone marrow stem cells into osteoblasts,[10,11] and alters the proliferation and differentiation capacity of $CD34^+$ cells.[12] Thus, it appears that the complex pathophysiology of GD may involve a wide array of cell types and processes.

It has been known for several decades that RBCs from GD patients also accumulate GlcCer.[13,14] However, RBC properties from GD patients have been investigated in a limited number of studies.[15-18] Among those is a hemorheologic study, which suggested a role for RBCs in the pathophysiology of GD.[16]

This study prompted us to further investigate the properties of GD RBCs using multiple techniques, in particular flow adhesion assays. We found that a significant proportion of GD RBCs exhibit abnormal shapes, adhere excessively to the endothelial vascular wall, and have abnormal rheologic properties. These results

Submitted July 10, 2012; accepted November 13, 2012. Prepublished online as *Blood* First Edition paper, December 3, 2012; DOI 10.1182/blood-2012-07-442467.

*E.C., P.C., C.L.V.K., and C.M. contributed equally to this work.

The online version of this article contains a data supplement.

The publication costs of this article were defrayed in part by page charge payment. Therefore, and solely to indicate this fact, this article is hereby marked "advertisement" in accordance with 18 USC section 1734.

indicate that GD encompasses an overlooked erythrocytopathy. They suggest the involvement of RBCs in ischemic events occurring in GD, including infarcts of spleen, bone, and AVN, as well as in the process leading to the appearance of pathogenic Gaucher cells in several organs.

Methods

Patients and blood samples

Blood samples were collected from 22 GD patients (10 men and 12 women; mean age 29 years) and 27 healthy volunteers age 20-years-old or more (CTR; 15 men and 12 women; mean age 33 years). The patients were recruited prospectively between July 2009 and February 2012. They were not under enzyme replacement therapy (ERT) when samples were collected. However, 2 of them had previously received ERT, which was discontinued 2 and 5 years before enrolment in this study. None of the GD patients had been splenectomised. Except for one patient who had the GD3 phenotype and another one with the D409H/D409H genotype usually associated with neurologic signs, all patients had the GD1 phenotype (n = 20). Seven patients had significant clinical or radiologic skeletal involvement (other than deformation of bones or medullar infiltration). On the whole, the studied population was representative of the French GD population and was distributed in 2 groups composed by 13 pediatric patients and 9 adult patients. GD was moderately severe as 12/22 patients enrolled in this study met the criteria for ERT. Detailed clinical information is available in Table 1.

Giemsa-stained blood smears were performed in CTR and GD, and RBCs with abnormal morphologies were quantified. This study and other experiments were done with RBCs from children and adult GD patients with various genotypes. In our experiments, these genotypes were equally distributed between those usually associated with a severe and those usually associated with a mild phenotype, except for the deformability study (*df*) in which 6/7 involved patients have a "severe" genotype.

GluCerase activity and expression during erythropoiesis

Peripheral blood mononuclear cells were isolated and erythroblasts were expanded and differentiated, as described.[19] Aliquots were taken daily during the 7-day differentiation from proerythroblasts to reticulocytes. Cells were washed twice in ice-cold PBS, lysed in 20mM Tris-HCl pH 8.0, 137mM NaCl, 10mM EDTA, 100mM NaF, 1% (vol/vol) Nonidet P-40, 10% (vol/vol) glycerol, 10mM Na_3VO_4, 2mM PMSF, 1% (vol/vol) protease inhibitor cocktail set V (Calbiochem), and nuclei were removed through centrifugation (15 700*g*, 10 minutes, 4°C). Proteins were analyzed by Western blotting using mouse antibodies against band 3 (BRIC 170, IBGRL) and Rho-GDI (Transduction Labs), and a rabbit antibody against GluCerase (Sigma-Aldrich). For GluCerase activity, 0.5×10^6 cells/experiment were washed once in PBS and resuspended in PBS with 4% fetal calf serum (FCS). Flow cytometry analysis of intracellular GC activity was performed using the fluorogenic GluCerase substrate 5′pentafluorobenzoylaminofluorescein-di-β-D-glucoside (PFB-FDGlu, Life Technologies). Cells were incubated with 1mM of the GluCerase substrate or DMSO as control, for 30 minutes at 37°C. The reaction was stopped with addition of 3 mL of ice-cold PBS and PFB-F fluorescence was measured by FACS.[20] When necessary, cells were pre-incubated for 1 hour at 37°C with 500μM conduritol B epoxyde (CBE), a GluCerase inhibitor.

Adhesion assay

RBC adhesion assays were performed using a plate flow chamber and ibiTreat or uncoated microslide $I^{0.2}$ Luer (Ibidi). For RBC adhesion on human microvascular endothelial cells (HMEC-1) under semistatic conditions, HMEC-1 were cultured in MCDB131 medium (Invitrogen) containing 15% FCS (Invitrogen), 10 ng/mL EGF (Sigma-Aldrich), 1 ng/mL hydrocortisone (Sigma-Aldrich), and antibiotics. HMEC-1 cells were activated with TNFα (10 ng/mL) for 48 hours at 37°C. The day before the adhesion assay, cells were plated at a concentration of 16×10^6 cells/mL, and medium was changed via a peristaltic pump system every 4 hours. RBCs were washed and resuspended in Hanks buffer supplemented with 0.2% bovine serum albumin (BSA) at 0.5% hematocrit (Hct). The RBC suspension was perfused through the HMEC-1–coated microslide at a flow-rate of 0.2 dyn/cm^2 for 2 minutes. Then, the flow-rate was stopped during 45 minutes at 37°C to allow RBC adhesion to endothelial cells. The flow-rate was restarted, followed by a 5-minute wash of nonadherent RBCs at 0.2 dyn/cm^2 and 3-minute washouts from 0.2 to 3 dyn/cm^2. After each wash, adherent RBCs were counted in 6 representative areas by microscopy, using the Optimas 6.1 image analysis system (Media Cybernetics). For RBC adhesion to laminin, 10 μg of laminin α5 chain from human placenta (Sigma-Aldrich) was immobilized on uncoated microslide at 4°C overnight. Washed RBCs were resuspended at 0.5% Hct, and the suspension was perfused through the microslide at a flow rate of 0.3 dyn/cm^2 for 5 minutes at 37°C. After nonadherent cells were washed out for 5 minutes at 0.3 dyn/cm^2, flow rate was progressively increased from 0.4 to 1.6 dyn/cm^2 for 3 minutes each and adherent RBCs were counted as described. To compare RBC adhesion to laminin and fibronectin, laminin (10 μg) and human plasma fibronectin (7 μg; Sigma-Aldrich) were immobilized on microslides at 4°C overnight. Perfusion was performed at 0.2 dyn/cm^2 for 5 minutes. After a 5-minute wash, a shear stress of 0.4 dyn/cm^2 was applied and gradually increased from 1 to 4 dyn/cm^2 every 2 minutes. After each wash, adherent cells were counted in 11 representative areas using the AxioObserver Z1 microscope and AxioVision 4 analysis software (Carl Zeiss). Images of the same areas were obtained throughout each experiment using the "Mark and Find" module of AxioVision analysis software.

Immunofluorescence studies of HMEC-1 and adherent RBCs

To confirm laminin expression, HMEC-1 were activated with TNFα, cultured for 48 hours on microslides, and fixed for 20 minutes with 4% paraformaldehyde. After permeabilization for 10 minutes with 0.5% Triton X-100, HMEC-1 were incubated with antilaminin α5 chain (mAb 4C7, 1:40) for 1 hour at room temperature (RT) as previously described.[21] Microslides were washed with PBS-0.5% BSA and incubated with an AlexaFluor488–conjugated anti–mouse antibody (1:200) for 1 hour at RT. Microslides were examined by confocal microscopy using a Nikon EC-1 system equipped with 60×/1.4 NA and 100×/1.30 objectives. To visualize RBC morphology and Lu/BCAM expression pattern during the adhesion process, RBCs were fixed after washouts at 1 or 4 dyn/cm^2 for 20 minutes with 1% formaldehyde (Merck) and 0.025% glutaraldehyde (Sigma-Aldrich). RBCs were rinsed in PBS, incubated with F241 anti-Lu mAb (1:5000 in Dako Dakocytomation) for 1 hour at RT. Microslides were washed with Dako and incubated with AlexaFluor 488–conjugated anti–mouse antibody (1:200) for 1 hour at RT. To perform Lu/BCAM and α1β1-spectrin staining, RBCs were fixed for 20 minutes, permeabilized for 10 minutes in 0.5% Triton X-100, and incubated with F241 anti-Lu mAb and rabbit anti–α1β1-spectrin (obtained by immunization of rabbits with β1-spectrin purified chain) diluted in Dako for 1 hour at RT. RBCs were washed with Dako and incubated with AlexaFluor 488–conjugated anti–mouse antibody and AlexaFluor 568–conjugated anti–rabbit antibody (Invitrogen), respectively.

Flow cytometry

The expression of CD36, CD49d, CD29, and CD242 was assessed using specific monoclonal antibodies (Becton Dickinson). The percentage of reticulocytes in blood samples and the expression of Lu/BCAM were determined using thiazole orange dye (Reticount, BD Bioscience) and anti-Lu/BCAM mAb F241,[22] respectively. Acquisition and analysis were performed with the BD FACS Canto II flow cytometer (BD Bioscience) and with the BD FACS Diva software (Version 6.1.2).

To detect GluCerase activity by FACS, HEL cells (human erythroleukemia cells) or control RBCs were pretreated or not with CBE (100 mM, Sigma-Aldrich) for 1 hour, and incubated 30 minutes at 37°C in the presence of 1mM of PFB-FDGlu or DMSO as described.[20]

Table 1. Clinical and biologic parameters of the studied patients

Pat. no.	Age (y)	Age at diagnosis (y)	ERT start (age in y)	SMG	HMG	Clinical skeletal manifestations	Radiologic (MRI) skeletal manifestations	Hb (g/dL)	MCV (fL)	Platelet count (× 10^9/L)	Chitotriosidase activity (nmol/h/mL)	Ferritinemia (μg/L)	Gammaglobulinemia (g/L)	Genotype	Transferrin saturation percentage	Performed experiments
1	7	4	yes (7)	+	+	−	−	13.4	74	77	18 600	66	6,3	N370S/L444P	NA	*ah, al, e, p, m, df, hr*
2	5	2	no	+	+	−	−	11.4	77	91	7400	254	21	NA	NA	*al, e, p, m, hr*
3	8	2	yes (8)	+	+	−	−	12	75	131	13 300	148	10.5	N370S/1263del55	27	*ah, al, e, p*
4	7	4	no	+	+	−	−	10.8	74	81	4500	331	22	N370S/1265-1317del55	11	*ah, al, e, p*
5	12	11	yes (12)	+	−	bone pains	BI	10.8	80	100	11 250	498	10.9	NA	14	*ah, al, e, p*
6	11	11	no	+	+	−	−	11.8	74	84	11 900	348	13	?/?	NA	*ah, al, e, p , m , hr*
7*	3	3	yes (3)	+	+	−	−	9.9	56	178	24 450	19	6.65	R163X/I260M	5	*ah, al, e, p, m, df*
8	16	7	no	+	−	−	−	11.1	91	106	2780	419	10.9	N370S/?	24	*ah, al, e, p, m*
9	16	7	no	+	−	−	−	11.5	91	114	2260	437	11.1	N370S/?	18	*ah, al, e, p, m*
10	21	12	yes (22)	+	−	−	VBC	13.9	84	69	23 600	638	10.5	N370S/?	NA	*ah, al, e, p, m, hr*
11	1	1	yes (1)	+	+	−	−	11.5	67	99	25 100	214	11.2	D409H/D409H	NA	*m, hr, df*
12	63	57	yes (64)	+	+	−	−	12.8	84	104	7750	2141	11.9	N370S/?	22	*ah, al, e, p*
13	77	77	yes (78)	+	+	bone pains	BI	14.2	91	152	6200	1145	10.1	NA	55	*ah, al, e, p*
14	64	64	no	+	−	−	−	13.6	91	145	6700	578	11.5	N370S/N370S	NA	*ah, al, e, p, m, hr*
15	32	32	yes (33)	+	−	−	BI	16.1	81	172	800	771	10.5	N370S/N370S	NA	*ah, al, e, p*
16	67	67	yes (67)	+	+	−	BI	11.9	88	35	22 000	2500	12	N370S/L444P	24	*al, e, p, df*
17	45	45	yes (45)	+	−	−	−	15,3	86	101	1900	201	7.5	N370S/D218A	27	*ah, al, e, p, df*
18	47	47	no	+	−	−	NA	11	76	136	5250	18	21.7	N370S/N370S	NA	*ah, al, e, p, m, df*
19	29	9	yes (27)	+	+	−	−	15.8	90	150	NA	575	15.5	N370S/L444P	30	*al, e, p, m, df*
20	49	49	no	+	+	−	BI	12.5	89	102	36 500	308	15.2	NA	30	*m, hr*
21	29	6	no	+	−	bone pains	BI	12	84	143	5**	1008	14.2	N370S/N370S	24	*m, hr*
22	42	42	no	−	−	−	−	13.2	87	148	790	99	14.5	N370S/N370S	28	*m, hr*

ERT start (age in years): "no" means that the patient did not and still does not meet the criteria for ERT; "yes" is used for patients who did not receive ERT prior to our study and who started ERT due to GD severity either at the time of blood sampling or during the months following the study. Clinical skeletal manifestations: "+" indicates patients who experienced bone pains or at least 1 bone crisis. Radiologic (MRI) skeletal manifestations: bone deformations and medullary infiltration were considered insignificant findings for our study ("−" was used in this case); we used "BI" for patients whose skeletal MRI revealed at least 1 bone infarct, either painful or not in the disease history, and "VBC" for vertebral body collapse". Biologic parameters (ie, hemoglobinemia, MCV, platelet count, chitotriosidase activity, ferritinemia, and gammaglobulinemia, transferin saturation percentage) reported here are the results of the last recorded data, usually obtained the day of blood sampling for the study or a few weeks before. Genotype: "?" indicates the mutation was not identified despite screening of the most frequent mutations of the *GBA* gene. Performed experiments: *ah* adhesion to HMECs, *al* adhesion to laminin, *e* Lu/BCAM expression, *p* Lu/BCAM phosphorylation, *m* RBC morphologies, *df* membrane deformability, *hr* hemorheology.

SMG indicates splenomegaly; HMG, hepatomegaly; Hb, hemoglobin; and MCV, mean corpuscular volume.

*This patient has type 3 Gaucher disease.

**This patient has a constitutional chitotriosidase deficiency.

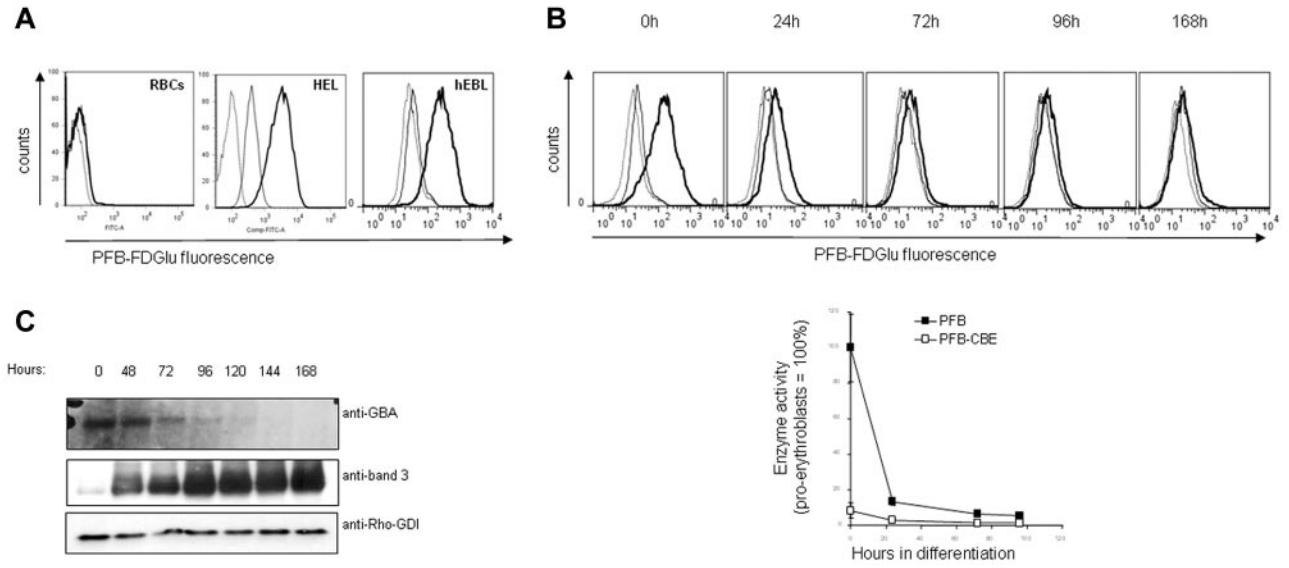

Figure 1. GC activity and expression in RBCs and during erythropoiesis. Erythroblasts expanded from peripheral blood mononuclear cells (PBMCs) were differentiated as indicated in "Methods." (A) GC activity was detected in human primary erythroblasts, but not in RBCs. GC activity was detected by flow cytometry, using cells treated with the PFB-FDGlu substrate (1mM) or DMSO for 30 minutes. The fluorescence histograms were overlaid to indicate the relative fluorescence levels of each sample. The dotted line represents DMSO-treated cells, the bold line represents cells incubated with the PFB-FDGlu substrate, and the straight line represents cells pretreated with the GC inhibitor CBE (1 hour, 1mM) before substrate incubation. (B) GC activity is rapidly decreasing during erythroblast differentiation. PFB-FDGlu substrate geometric mean fluorescence intensity (MFI) was measured at the indicated time points, and was normalized to the activity of GC in erythroblasts that was set at 100%. Standard deviation represents the variation between 4 independent experiments. The histogram overlays show representative figures of GC activity during erythroblast differentiation (dotted line = DMSO-control; bold line = PFB-FDGlu substrate; straight line = PFB-FDGlu substrate + CBE). (C) Aliquots were taken at the indicated time points and proteins were separated by SDS-PAGE. Blots were stained with antibodies against GC and band 3, and with an antibody to Rho-GDI as a loading control.

Phosphorylation status of Lu/BCAM in GD RBCs

The phosphorylation of Lu/BCAM was assessed as previously described.[23] Briefly, RBCs (200 μL) were washed and incubated in 2 mL phosphate-free medium for 4 hours at 35°C and 5% CO_2. After additional washes, RBCs were resuspended in 2 mL phosphate-free medium supplemented with orthophosphate ^{32}P (300 μCi) and incubated overnight at 35°C. RBCs were washed twice with cold PBS and lysed with lysis buffer supplemented with protease (Roche Diagnostics) and phosphatase inhibitor cocktails (Sigma-Aldrich). After overnight immunoprecipitation of Lu/BCAM with anti-Lu^b (clone LM342, from Dr R. H. Fraser, Regional Donor Center, Glasgow, United Kingdom) and protein A-Sepharose CL4B beads (Roche Diagnostics), the immunoprecipitates were washed and analyzed by SDS-PAGE, followed by protein transfer on nitrocellulose membranes. Lu/BCAM phosphorylation was quantified using the FujiFilm BAS-1800II PhosphoImager and Multi Gauge Version 3.0 software. Total immunoprecipitated Lu/BCAM was quantified by Western blotting using a biotinylated anti-Lu antibody (R&D Systems) and Quantity One Version 4.5.2 software (Biorad).

Hemorheology, hematologic, and biochemical analyses

Blood samples were immediately used for measurements of hemoglobin concentration, Hct, mean corpuscular volume (MCV), mean corpuscular hemoglobin concentration (MCHC), and platelet and white blood cell counts. Trisodium citrate blood samples were used for measurements of fibrinogen and von Willebrand factor antigen (VWF Ag test kit) levels. All hemorheologic measurements[24] were carried out within 4 hours of the venipuncture to avoid blood rheologic alterations[25] and after complete oxygenation of the blood.[24] We followed the guidelines for international standardization of blood rheology techniques/measurements and interpretation.[24] Blood viscosity was determined at native Hct, at 37°C and at various shear rates using a cone/plate viscometer (Brookfield DVIII+ with CPE40 spindle, Brookfield Engineering Labs). We used a "loop" protocol where the shear rate started at 22.5 $seconds^{-1}$, was increased every 30 seconds until 225 $seconds^{-1}$, at which point it was decreased every 30 seconds to the initial shear rate. This loop protocol provides information on the effects of RBC aggregation and deformability properties on blood viscosity during the dynamic transition from a given shear rate to another shear rate. RBC deformability (EI, elongation index) was determined at 37°C at 9 shear stresses ranging from 0.30 to 30 Pa by laser diffraction analysis (ektacytometry), using the laser-assisted optical rotational cell analyzer (LORCA, RR Mechatronics). The value of 3.00 Pa is often considered as the threshold between low/moderate shear and high shear stress values. At less than 3.00 Pa, RBC deformability is more dependent on the ability of the RBC membrane to deform under shear, whereas at more than 3.00 Pa RBC deformability mainly depends on the internal viscosity of the cells.[24] RBC aggregation was determined at 37°C via syllectometry, (ie, laser backscatter versus time, using the LORCA) after adjustment of the Hct to 40%, and was reported as the aggregation index (AI). The RBC disaggregation threshold (γ), that is, the minimal shear rate needed to prevent RBC aggregation or to breakdown existing RBC aggregates, was determined using a reiteration procedure.[26]

Statistical analyses

Results are presented as the mean ± SEM. Mann-Whitney test was used to compare RBC morphology, RBC adhesion to HMEC-1 and laminin at every shear stress, Lu/BCAM expression and phosphorylation state, RBC membrane properties during flow experiment, RBC aggregation and disaggregation, and RBC deformability at every shear stress between the CTR and GD groups. A 1-way analysis of variance (ANOVA) was used to compare the blood viscosities determined during the 2 steps of the loop protocol between the 2 groups for any given shear rate, and RBC adhesion to laminin and fibronectin between the 2 groups. Pairwise contrasts were used to determine differences. Statistical significance was established at $P < .05$.

Results

GluCerase is expressed and active in erythroid progenitors but not in late differentiation and mature red cells

GluCerase activity was measured in normal RBCs and erythroid progenitors. Flow cytometry analysis using a specific fluorogenic

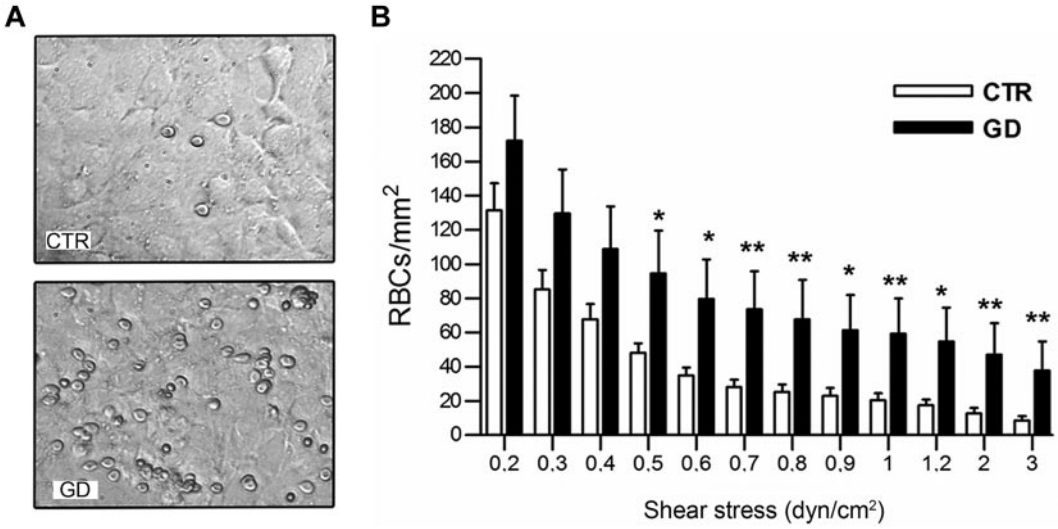

Figure 2. Adhesion of GD and CTR RBCs to HMEC-1 endothelial cells under flow conditions. (A) Typical microscopic images showing that more GD RBCs adhere to HMEC-1 monolayer than healthy volunteer RBCs at 1 dyn/cm^2 flow rate. (B) Number of RBCs remaining adherent to HMEC-1 after inflow at 0,2 dyn/cm^2 and washout at increasing shear stresses. Blood samples were from 12 healthy CTRs and 15 GD patients. Bars denote SEM (*$P < .05$; **$P < .01$; Mann-Whitney test).

GluCerase substrate failed to reveal GluCerase activity in RBCs (Figure 1A), which is in agreement with the absence of lysosomes in mature RBCs. In contrast, GluCerase activity was clearly detected in the erythroleukemic cell line HEL and in human primary proerythroblasts, suggesting that, in case of GluCerase deficiency, the accumulation of GlcCer would occur at early stages during erythroid differentiation (Figure 1A). We then assessed the GluCerase activity and expression during in vitro erythropoiesis.[19] The enzyme activity was high in proerythroblasts, but decreased sharply within the first 72 hours of differentiation and was absent at later stages (Figure 1B). In agreement with the enzyme activity, Western blot analysis revealed that GluCerase was expressed only at the earliest stages of erythroid differentiation (proerythroblast to basophilic stage; Figure 1C).

Abnormal morphologies of GD RBCs

RBC morphology was examined on Giemsa-stained peripheral blood smears from CTR (n = 12) and GD (n = 14) individuals. We observed significantly greater proportion of abnormal RBC shapes in GD patients (2.90% ± 1%) compared with CTR samples, with presence of dacryocytes ("tear drop" cells), elliptocytes, echinocytes, and schistocytes (supplemental Figure 1, available on the *Blood* Web site; see the Supplemental Materials link at the top of the online article). This confirms a previous observation,[17] and suggests that GD RBCs may have membrane or cytoskeleton (or both) abnormal properties with potential functional consequences.

Enhanced adhesion of GD RBCs to HMEC-1 and laminin α5

The adhesive properties of GD RBCs (n = 15) versus CTR RBCs (n = 12) to HMEC-1 were examined under flow. GD RBCs were significantly more adherent than CTR RBCs (Figure 2A) at all shear stresses, ranging from 0.5 to 3 dyn/cm^2 ($P < .05$ or $< .01$; Figure 2B).

Laminin α5 is known to facilitate the adhesion of RBCs to HMEC-1.[21] Immunofluorescence studies showed that laminin α5 was expressed at the cell surface, and on the basal and apical sides of HMEC-1 (data not shown). The adhesion of GD (n = 18) and CTR RBCs (n = 18) on microslides coated with purified laminin α5 was analyzed under flow. GD RBCs adhered significantly better than CTR RBCs at all shear stresses ($P < .05$ or $< .01$; Figure 3A). However, neither GD RBCs nor CTR RBCs adhered to fibronectin (Figure 3B). These data indicate that GD RBCs exhibit enhanced

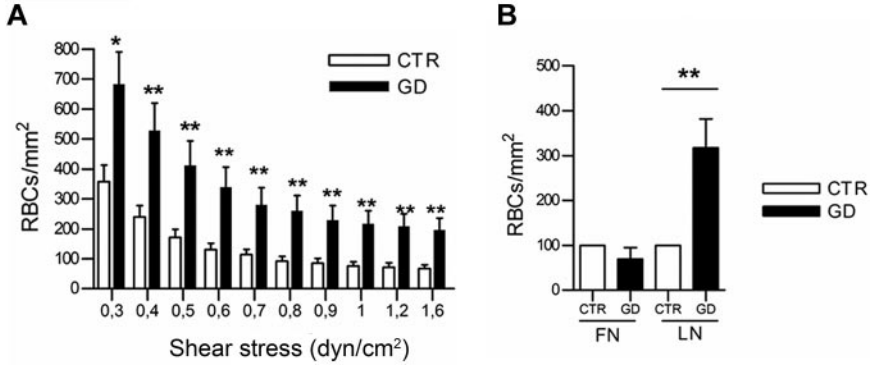

Figure 3. Adhesion of GD and CTR RBCs to purified laminin α5 under flow conditions. (A) Blood samples were from 18 healthy CTRs and 18 GD patients. Number of RBCs remaining adherent to purified laminin α5-coated microslide after inflow at 0.3 dyn/cm^2 and washout at increasing shear stresses. Bars denote SEM (*$P < .05$; **$P < .01$; Mann-Whitney test). (B) Increased GD RBC adhesion compared with CTR RBCs is specific to laminin α5 and not to fibronectin (after inflow at 0.2 dyn/cm^2 and increasing washout until 1 dyn/cm^2, $P < .01$; ANOVA followed by Dunn multiple comparison test). Blood samples were from 4 healthy CTRs and 4 GD patients. GD RBCs were more adherent to laminin than CTR RBCs.

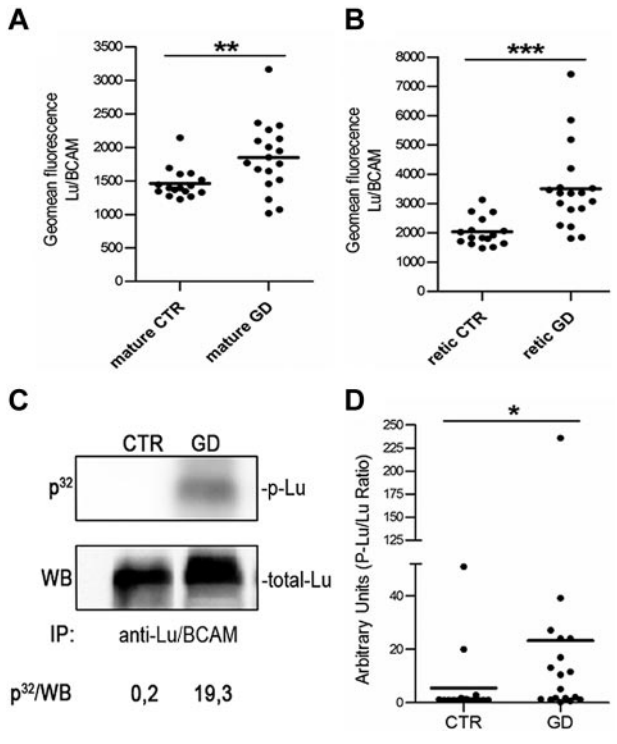

Figure 4. Expression and phosphorylation status of Lu/BCAM in GD and CTR RBCs. (A-B) Lu/BCAM cell-surface expression was measured in RBCs from 16 CTRs and 18 GD patients using anti-Lu/BCAM monoclonal antibody F241 and flow cytometry. Compared with control RBCs, a higher geometric fluorescence intensity was observed in mature RBCs (***$P < .0001$; Mann-Whitney test [A]) and reticulocytes of GD patients (**$P < .01$; Mann-Whitney test [B]). Horizontal lines represent medians. (C) Typical results of radiophospholabeling of GD and CTR RBCs followed by immunoprecipitation of Lu/BCAM protein by a specific anti-Lu antibody. The phosphorylated proteins were detected using phosphoimager and the corresponding total immunoprecipitated Lu/BCAM proteins were quantified by Western blot (WB) using a biotinylated anti-Lu/BCAM antibody. The P/WB ratio (arbitrary units) estimates the proportion of phosphorylated Lu/BCAM protein. (D) P/WB ratio obtained with CTR (n = 16) and GD (n = 18) RBCs. Horizontal lines represent medians. We observed more phosphorylated Lu/BCAM in GD RBCs than in CTR RBCs (*$P = .0113$; Mann-Whitney test).

adhesion to endothelial cells via laminin α5 expressed on endothelial cells.

Lu/BCAM expression and phosphorylation is increased in GD RBCs

Flow cytometry was used to investigate the expression of adhesion molecules known to be involved in RBCs-endothelium/laminin interactions.[27] We used specific adhesion molecule antibodies in association with Reticount staining to discriminate membrane protein expression in reticulocytes and in mature RBCs. No significant differences were observed for the adhesion molecules CD36, CD49d (α4 integrin), CD29 (β1 integrin), and CD242 (I-CAM4) between reticulocytes or erythrocytes from GD and CTR samples (data not shown). In contrast, the expression of CD239 (Lu/BCAM), the unique receptor of laminin α5 on RBCs and erythroblasts[28] was in average significantly higher in circulating mature GD RBCs ($P < .01$) and reticulocytes ($P < .001$) than in CTR cells (Figure 4A-B), although the expression levels varied widely between GD samples. A correlation was found between Lu/BCAM geometric fluorescence intensity and percentage adhesion to laminin α5 ($\rho = 0.64$, $P < .01$; not shown).

Because Lu/BCAM activation by phosphorylation enhances the adhesion of RBCs to laminin α5,[23,28] we performed radiophospholabeling experiments to determine the phosphorylation status of Lu/BCAM in GD (n = 18) versus CTR (n = 16) RBCs. As shown in Figure 4C and D, a significant increase in Lu/BCAM phosphorylation was observed in immunoprecipitates from GD RBCs compared with those from CTR RBCs ($P < .05$). These results indicate that Lu/BCAM is highly expressed and is activated in the RBCs from GD patients.

Abnormal membrane properties of GD RBCs during flow adhesion

To more precisely analyze the membrane properties of GD RBCs during adhesion to laminin α5, confocal imaging was performed during adhesion experiments under flow. At 1 dyn/cm^2, CTR RBCs were elongated and underwent a deformation of their membrane, with RBCs exhibiting a typical racket shape (Figure 5A). In contrast, GD RBCs did not change shape, suggesting reduced membrane deformability. Counting RBCs with a racket shape at 1 dyn/cm^2 indicated that the proportion of deformed RBCs was significantly higher in CTR RBCs (~70%) compared with GD RBCs (~ 40%; $P < .01$; Figure 5A). When applying higher shear stress (4 dyn/cm^2), GD RBCs exhibited frequent and elongated membrane tethers (Figure 5B), with a length that was significantly greater in GD than in CTR RBCs ($P < .001$; Figure 5B). These data suggest uncoupling of the membrane lipid bilayer from the cytoskeleton in GD RBCs.[29,30] The segregation between the membrane lipid bilayer and the spectrin-based membrane skeleton under high shear stress was confirmed by immunolabeling, showing that α1β1 spectrin, in contrast to Lu/BCAM, was not detected at the level of the membrane tether (Figure 5C). These findings suggest that the properties of the GD RBCs membrane may be altered in a way that prevents cell deformation and favors membrane dissociation from the cytoskeleton on shear stresses.

Abnormal hemorheologic properties of GD RBCs

RBC hemorheologic properties of 9 GD and 11 CTR blood samples were analyzed. GD RBC deformability was reduced compared with CTR RBCs at 0.3, 0.53, 0.95, 1.69, and 3.00 Pa ($P < .05$ or $< .01$, or $< .001$; Table 2). At more than 3.00 Pa, the deformability was no longer different between the 2 groups. In addition, RBC aggregation was higher in GD patients than in CTR ($P < .05$; Figure 6A), as was the RBCs disaggregation threshold ($P < .05$; Figure 6B). Blood viscosity was greater in GD patients than in CTR at every shear rate during the increasing phase of the loop ($P < .05$; Figure 6C curve 1), but not during the decreasing phase of the loop (Figure 6C curve 2). Blood viscosity at a given shear rate decreased between the incrementing and the decreasing phases of the loop protocol in the GD group ($P < .05$ or $< .01$; Figure 6C). In summary, the "up" (curve 1) and "down" (curve 2) curves did not coincide in GD patients and this hysteresis loop, denoting thixotropy, reflects the effects of increased RBC aggregation on blood viscosity.

The hematologic and biochemical parameters were measured in the same GD patients. Hb (12.59 ± 0.32 g/dL) and Hct (36.42% ± 0.91%) levels were within the normal range, except for 3/9 patients who were slightly anemic, with microcytosis because of lower MCV values. The mean MCV of all 9 GD patients was within the lowest values of the normal range (80.8 ± 2.7 fL). All GD patients exhibited thrombocytopenia (106 ± 31 10^9/L). Neither fibrinogen (2.51 ± 0.17 g/L, normal range 1.5 to 4 g/L), nor VWF antigen (89.41% ± 12.27%, normal range 50% to 150%) values were out of the normal ranges. No correlation between RBC

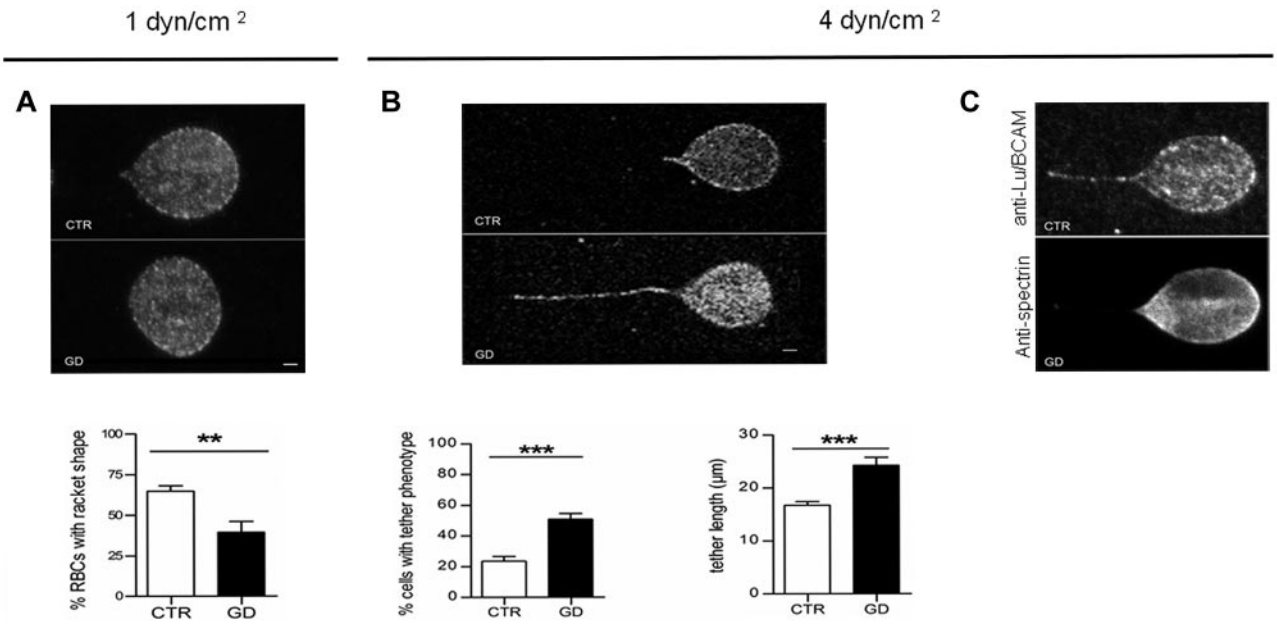

Figure 5. Confocal imaging of adherent GD and CTR RBCs to laminin α5 at different shear stresses. (A) Typical microscopic images showing the shape of adherent RBCs from 7 healthy CTRs and 7 GD patients at 1 dyn/cm^2. The flow is from the left to the right. Lu/BCAM cell-surface expression was visualized by immunofluorescence using the monoclonal antibody F241 and confocal microscopy. Percentage of adherent RBCs with racket shape after inflow at 0.2 dyn/cm^2 and increasing washout until 1dyn/cm^2 was higher in CTR RBCs compared with GD RBCs ($P < .01$, Mann-Whitney test). (B) Same experiments as in panel A but with final washout at 4 dyn/cm^2. GD RBCs frequently exhibited typical tether shape. Bars scales represent 1 μm. RBCs from GD patients exhibited more frequently a tether shape than CTR RBCs (***$P < .0001$). RBCs from GD patients exhibited longer tethers than CTR RBCs. Tether measurement was performed on 30 cells per condition (***$P < .0004$). (C) Same experiments as in panel B but GD RBCs were double-stained with anti-Lu/BCAM (top panel) or anti-spectrin (bottom panel) antibodies.

aggregation properties and VWF antigen (RBC aggregation/VWF, $\rho = -0.29$, $P = .50$; RBC disaggregation threshold/VWF, $\rho = -0.59$, $P = .11$) or fibrinogen levels (RBC aggregation/fibrinogen, $\rho = -0.18$, $P = .71$; RBC disaggregation threshold/fibrinogen, $\rho = -0.56$, $P = .15$) was found in GD patients.

Altogether, our findings indicate that GD RBCs exhibit abnormal deformability at low shear stress, aggregation, and disaggregation properties as well as blood viscosity.

Discussion

In this study, we investigated the potential role of RBCs in the pathophysiology of GD. We confirm the hemorheologic alterations of GD RBCs, and demonstrate for the first time their enhanced adhesive properties. During flow adhesion experiments, we observed an abnormal behavior of GD RBCs compared with CTR RBCs. At 1 dyn/cm^2 (ie, 0.1 Pa), GD RBCs adherent to laminin displayed reduced deformability. This apparent low deformability was confirmed by hemorheologic experiments, revealing that the deformability of CTR RBCs was 3-fold greater than that of GD RBCs at the lowest shear stress applied (ie, 0.3 Pa). These results, obtained with RBCs from nonsplenectomised GD patients, are in contrast to those from a previous study reporting reduced deformability of RBCs from splenectomised but not from nonsplenectomised GD patients.[16] In the study by Bax et al, the authors used the St George blood cell filtrometer to measure the RBC filtration rate at a shear stress which is far more than the shear stresses commonly found in the microcirculation.[16] RBC deformability in our study was measured by what is considered as the gold standard test, allowing the evaluation of this parameter under more physiologic flow conditions. Our results were different from those of Bax et al at low-moderate shear stresses, but were no longer different at shear stresses more than 3.00 Pa.[16] Therefore, the results obtained with RBCs from nonsplenectomised GD patients in both studies are not contradictory. Our data further indicate that membrane elasticity rather than internal viscosity probably determines the loss of GD RBCs deformability.

Hemorheologic data suggest membrane alterations in GD RBCs, and may explain the abnormal RBC shapes in GD observed in this and previous studies.[17] Here, we confirm that a significant proportion of RBCs from GD patients with an intact spleen and not under ERT have abnormal shapes. Schistocytes probably result from RBC fragmentation passing through microvessels lined with mesh of fibrin strands. This raises the issue of a potential correlation between the presence of schistocytes and markers of intravascular hemolysis that were not assessed in this study. Other abnormal shapes indicated that the properties of the membrane, the skeleton-based membrane, or both could be altered in GD RBCs.

Our results are in agreement with previous findings demonstrating increased aggregation of RBCs from splenectomised and nonsplenectomised patients.[15,18] The mechanisms of RBC hyperaggregation in GD patients are poorly understood, but could involve both plasma factors[15,18] and intrinsic cellular factors.[15] Because

Table 2. RBC deformability (EI) at several shear stresses (Pa) in control subjects (CTR) and Gaucher patients (GD)

	0.30	0.53	0.95	1.69	3.00	5.33	9.49	16.87	30.00
CTR	0.06 ± 0.01	0.08 ± 0.01	0.16 ± 0.02	0.26 ± 0.02	0.36 ± 0.02	0.44 ± 0.01	0.50 ± 0.01	0.55 ± 0.01	0.59 ± 0.01
GD	0.02 ± 0.02***	0.06 ± 0.01**	0.13 ± 0.03**	0.23 ± 0.03*	0.33 ± 0.03*	0.42 ± 0.02	0.50 ± 0.02	0.55 ± 0.01	0.58 ± 0.01

Difference between the 2 groups (*$P < .05$; **$P < .01$; ***$P < .001$).

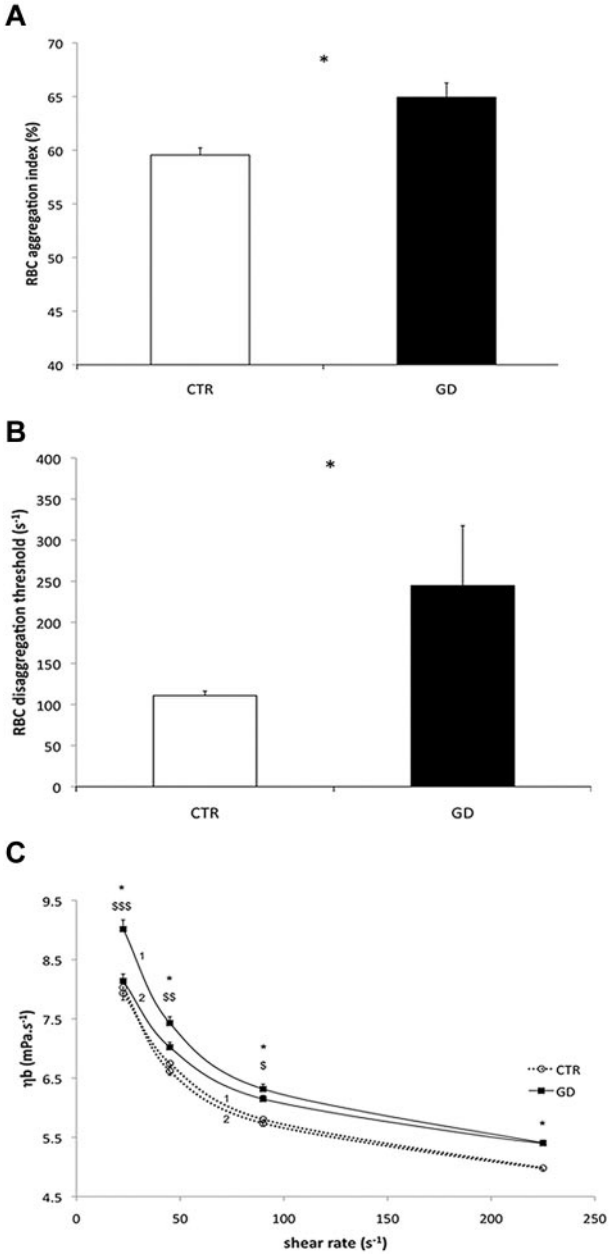

Figure 6. Hemorheologic analyses of GD and CTR RBCs. For all the studies, blood samples were from 11 healthy CTRs and 9 GD patients. (A) RBC aggregation in control CTR subjects and GD patients (*$P < .05$). (B) RBCs disaggregation threshold in CTR and GD patients (*$P < .05$). (C) Blood viscosity (ηb) in CTR and GD patients at different shear rates. A loop protocol was used with shear rate increasing from moderate value to high value (curves 1), and then the shear rate was reduced (curves 2) to the initial value (see "Methods" for details). Difference between the 2 groups during the incrementing phase of the loop (curves 1; *$P < .05$). Difference between the value obtained during the incrementing phase of the loop protocol (curves 1) and the value obtained during the decreasing phase of the loop protocol (curves 2) in the GD group ($^{\$}P < .05$; $^{\$\$}P < .01$; $^{\$\$\$}P < .001$).

plasma levels of gammaglobulins, fibrinogen, and VWF antigen in our GD patients were within normal physiologic ranges and were not significantly correlated with RBC aggregation, cellular factors probably predominate.

In addition to hyperaggregation, we show for the first time that GD RBCs have an increased disaggregation threshold (2-fold greater) compared with CTRs. This means that the strength needed to disperse pre-existing RBC aggregates is higher in GD patients than in CTRs. Aggregation abnormalities of GD RBCs probably explain the measures of blood viscosity under shear transitions with marked hysteresis during the loop blood viscosity protocol.[31] The normalization of GD blood viscosity in the second part of the loop protocol is probably because most RBC aggregates progressively disaggregate during the incrementing shear rate phase, limiting the effects of RBC aggregation on blood viscosity when the shear rate returns to the initial low values. Both the reduced RBC deformability at low shear stress and the increased RBC aggregation may explain the increased thixotropic properties of blood in GD patients and may increase the risk of microcirculatory disorders. Increased aggregation properties of GD RBCs may increase flow resistance in low shear vascular regions or in the microcirculation where RBC aggregates need to be dispersed to allow single RBCs to enter and negotiate the small capillaries.[32] Thus, hemorheologic properties of GD RBCs are potential factors contributing to "vaso-occlusive like" events in this pathology.

In sickle cell disease (SCD), vaso-occlusive events are triggered by sickling of the RBCs in areas of low oxygen or in response to hemorheologic abnormalities and abnormal adhesion to the vascular wall.[33-35] The adhesion of affected RBCs slows down the RBCs transit time in the microcirculation and initiate vaso-occlusive crises.[36,37] These events occur in many organs, but they are particularly common in the bone.[38] We previously reported that Lu/BCAM, the unique receptor of laminin in RBCs and erythroblasts[28] mediates abnormal adhesion to laminin *α5* and to endothelial cells in SCD patients.[23,39,40] We demonstrated here a similar ability of GD RBCs to adhere to microvascular endothelial cells and to laminin *α5*. Lu/BCAM, but not CD36, α4β1 or ICAM-4 adhesion molecules, was highly expressed in circulating mature RBCs and reticulocytes from GD patients compared with healthy subjects. Whether other receptor/ligand partners are involved in the increase in GD RBC-endothelium adhesion requires further studies. Interaction between laminin *α5* and Lu/BCAM requires phosphorylation of the cytoplasmic domain of the receptor.[21,23,40] We observed enhanced phosphorylation of Lu/BCAM in GD RBC samples, which demonstrates that the protein is in an activated state. The signals responsible for this phosphorylation are unknown. It may result from increased shear stress or from other membrane alterations because of the underlying GluCerase deficiency. Lu/BCAM may mediate RBC adhesion to laminin α5-expressing cells, which combined with altered hemorheologic properties, may result in the increased risk for ischemic events in patients with GD.

The relatively limited number of studied patients and their relatively moderate phenotype, that is, absence of skeletal involvement at the time of blood sampling in most of them (only 7 untreated patients had radiologic or clinical skeletal manifestations), did not allow us to correlate RBC anomalies with the severity of GD. Larger studies may help define the role of RBC pathology in the phenotype of GD patients. Furthermore, CTR RBCs were from adult patients. Experiments performed with age-matched controls may possibly give different results. However, we could observe a tendency to higher adhesion to laminin with RBCs from patients with symptomatic bone damage and/or high chitotriosidase activity as compared with asymptomatic patients (not shown).

GD has long been considered as a primarily macrophage-specific glucosphingolipidosis. However, recent studies suggest that the accumulation of GlcCer in other cell types may have detrimental effects in GD.[10-12] Our study points to the direct involvement of erythroid cells in GD pathophysiology. Taken together, our data demonstrate that hemorheologic parameters and adhesion properties of GD RBCs are abnormal, indicating that GD

encompasses an "erythrocytopathy." Although the analogy between the "bone crises" and AVN of both GD and SCD is obvious,[5] vaso-occlusive events are by far less frequent in GD than in SCD. The hemorheologic differences, and many other nonerythrocytic factors specific to each condition, may account for the clinical differences between GD and SCD. However, hemorheologic, as well as adhesion similarities, may account for clinical similarities between both diseases.

We postulate that increased GD RBC adhesion might be related to the accumulation of GlcCer into RBC membranes[14] and the aberrant lipid membrane composition, causing membrane alterations and Lu/BCAM activation. This hypothesis is supported by the effect of D-PDMP, an inhibitor of GlcCer synthase, in cancer research. This compound induces a depletion of glycosphingolipids, and reduces the adhesion of B16 cancer cells to laminin, which can be counteracted by the addition of GlcCer in the culture medium.[41] We suggest that GlcCer could control the distribution of Lu/BCAM into RBCs by regulating the fluidity of the plasma membrane and/or the lateral distribution of Lu/BCAM, thereby controlling its activity.

In line with previous findings, we detected GluCerase activity in normal erythroblasts but not in circulating RBCs.[12] Thus, GlcCer accumulation could occur in the early stages of erythropoiesis. However, high GlcCer plasma levels are found in GD patients,[42,43] which raises the question of whether RBCs GlcCer overload may be caused by passive incorporation of GlcCer; this hypothesis needs to be further studied.

Beyond ischemic events, RBC properties may be responsible for their enhanced splenic destruction. Indeed, their low deformability and increased adhesion to the endothelium may slow down their passage through narrow splenic microvessels, and may even prevent them from passing through splenic capillaries. Hence, it is conceivable that the 3% RBCs with an abnormal shape, as well as RBCs exhibiting abnormal adhesion and hemorheologic properties, may be recognized by splenic macrophages and cleared from the circulating pool. Thus, RBCs could be the primary dysfunctional cells, leading to formation of Gaucher cells in the spleen. It may also be the case in the bone marrow where erythrophagocytosis is frequently reported,[17] and possibly in other organs containing resident macrophages. After they are formed, GlcCer-laden macrophages (Gaucher cells) that display abnormal properties[44,45] may induce further organ dysfunction depending on their specific environment. Hence, RBCs and interactions between RBCs and macrophages may be crucial in the pathogenesis of GD.

In summary, our study reveals that the RBCs from GD patients exhibit abnormal properties, including abnormal morphology, altered hemorheology, and increased adhesion to the endothelium, mainly mediated by laminin α5. These findings uncover an overlooked aspect in GD pathophysiology, and suggest that RBCs might be responsible for ischemic processes in GD. Another crucial step will be to determine whether ERT, which is usually efficient in preventing Gaucher symptoms, normalizes RBC parameters.

Acknowledgments

The authors thank Julien Picot and Sylvain Bigot for performing the flow cytometry analyses, and Aurélien Pichon and Wassim El Nemer for their help on hemorheologic and protein phosphorylation analyses. They thank Djazia Heraoui and Dr Jerôme Stirnemann for their support to collect GD patients, and Dr Caillaud (Laboratoire de Génétique Métabolique, hôpital Cochin) for her contribution to the update of genetic data. The authors also thank the patients with Gaucher disease and their families for their participation in the research project. They thank the Program d'Investissements d'Avenir from ANR and Shire France for financial support, and Dr Martine Torres for editorial assistance.

Authorship

Contribution: M.F., C.L.V.K., and C.M. designed the study; T.B.V., N.B., and C.M. took care of patients; T.B.V. and N.B. provided patient blood samples; M.F., E.C., P.C., N.A., and E.V.D.A. performed the experiments; M.F., P.C., Y.C., E.V.D.A., M.V.L., O.H., C.L.V.K., and C.M. analyzed the data; and M.F., P.C., Y.C., C.L.V.K., and C.M. wrote the paper.

Conflict-of-interest disclosure: The authors declare no competing financial interests.

Correspondence: Caroline Le Van Kim, Inserm U665, INTS, 6 Rue Alexandre Cabanel, 75015 Paris, France; e-mail: caroline.le-van-kim@inserm.fr; or Cyril Mignot, Service de Neuropédiatrie, Hopital Armand Trousseau, 26 rue du Dr Arnold Netter, 75012 Paris, France; e-mail: cyril.mignot@psl.aphp.fr.

References

1. Cox TM, Schofield JP. Gaucher's disease: clinical features and natural history. *Baillieres Clin Haematol.* 1997;10(4):657-689.
2. Grabowski GA. Phenotype, diagnosis, and treatment of Gaucher's disease. *Lancet.* 2008;372(9645):1263-1271.
3. Stowens DW, Teitelbaum SL, Kahn AJ, Barranger JA. Skeletal complications of Gaucher disease. *Medicine (Baltimore).* 1985;64(5):310-322.
4. Bembi B, Ciana G, Mengel E, Terk MR, Martini C, Wenstrup RJ. Bone complications in children with Gaucher disease. *Br J Radiol.* 2002;75(Suppl 1):A37-44.
5. Deegan PB, Pavlova E, Tindall J, et al. Osseous manifestations of adult Gaucher disease in the era of enzyme replacement therapy. *Medicine (Baltimore).* 2011;90(1):52-60.
6. Guggenbuhl P, Grosbois B, Chales G. Gaucher disease. *Joint Bone Spine.* 2008;75(2):116-124.
7. Rossi L, Zulian F, Stirnemann J, Billette de Villemur T, Belmatoug N. Bone involvement as presenting sign of pediatric-onset Gaucher disease. *Joint Bone Spine.* 2011;78(1):70-74.
8. Mikosch P. Miscellaneous noninflammatory musculoskeletal conditions. Gaucher disease and bone. *Best Pract Res Clin Rheumatol.* 2011;25(5):665-681.
9. Wenstrup RJ, Roca-Espiau M, Weinreb NJ, Bembi B. Skeletal aspects of Gaucher disease: a review. *Br J Radiol.* 2002;75(Suppl 1):A2-12.
10. Lecourt S, Vanneaux V, Cras A, et al. Bone marrow microenvironment in an in vitro model of Gaucher disease: consequences of glucocerebrosidase deficiency. *Stem Cells Dev.* 2012;21(2):239-248.
11. Mistry PK, Liu J, Yang M, et al. Glucocerebrosidase gene-deficient mouse recapitulates Gaucher disease displaying cellular and molecular dysregulation beyond the macrophage. *Proc Natl Acad Sci U S A.* 2010;107(45):19473-19478.
12. Berger J, Lecourt S, Vanneaux V, et al. Glucocerebrosidase deficiency dramatically impairs human bone marrow haematopoiesis in an in vitro model of Gaucher disease. *Br J Haematol.* 2010;150(1):93-101.
13. Erikson A, Forsberg H, Nilsson M, Astrom M, Mansson JE. Ten years' experience of enzyme infusion therapy of Norrbottnian (type 3) Gaucher disease. *Acta Paediatr.* 2006;95(3):312-317.
14. Nilsson O, Hakansson G, Dreborg S, Groth CG, Svennerholm L. Increased cerebroside concentration in plasma and erythrocytes in Gaucher disease: significant differences between type I and type III. *Clin Genet.* 1982;22(5):274-279.
15. Adar T, Ben-Ami R, Elstein D, et al. Aggregation of red blood cells in patients with Gaucher disease. *Br J Haematol.* 2006;134(4):432-437.
16. Bax BE, Richfield L, Bain MD, Mehta AB, Chalmers RA, Rampling MW. Haemorheology in Gaucher disease. *Eur J Haematol.* 2005;75(3):252-258.
17. Bratosin D, Tissier JP, Lapillonne H, et al. A cytometric study of the red blood cells in Gaucher disease reveals their abnormal shape that may be involved in increased erythrophagocytosis. *Cytometry B Clin Cytom.* 2011;80(1):28-37.
18. Zimran A, Bashkin A, Elstein D, et al. Rheological determinants in patients with Gaucher disease

and internal inflammation. *Am J Hematol.* 2004; 75(4):190-194.

19. van den Akker E, Satchwell TJ, Pellegrin S, Daniels G, Toye AM. The majority of the in vitro erythroid expansion potential resides in CD34(-) cells, outweighing the contribution of CD34(+) cells and significantly increasing the erythroblast yield from peripheral blood samples. *Haematologica.* 2010;95(9):1594-1598.
20. Lorincz M, Herzenberg LA, Diwu Z, Barranger JA, Kerr WG. Detection and isolation of gene-corrected cells in Gaucher disease via a fluorescence-activated cell sorter assay for lysosomal glucocerebrosidase activity. *Blood.* 1997;89(9):3412-3420.
21. Wautier MP, El Nemer W, Gane P, et al. Increased adhesion to endothelial cells of erythrocytes from patients with polycythemia vera is mediated by laminin alpha5 chain and Lu/BCAM. *Blood.* 2007;110(3):894-901.
22. Kroviarski Y, El Nemer W, Gane P, et al. Direct interaction between the Lu/B-CAM adhesion glycoproteins and erythroid spectrin. *Br J Haematol.* 2004;126(2):255-264.
23. Bartolucci P, Chaar V, Picot J, et al. Decreased sickle red blood cell adhesion to laminin by hydroxyurea is associated with inhibition of Lu/BCAM protein phosphorylation. *Blood.* 2010; 116(12):2152-2159.
24. Baskurt OK, Boynard M, Cokelet GC, et al. New guidelines for hemorheological laboratory techniques. *Clin Hemorheol Microcirc.* 2009;42(2):75-97.
25. Uyuklu M, Cengiz M, Ulker P, et al. Effects of storage duration and temperature of human blood on red cell deformability and aggregation. *Clin Hemorheol Microcirc.* 2009;41(4):269-278.
26. Hardeman MR, Dobbe JG, Ince C. The laser-assisted optical rotational cell analyzer (LORCA) as red blood cell aggregometer. *Clin Hemorheol Microcirc.* 2001;25(1):1-11.
27. Cartron JP, Elion J. Erythroid adhesion molecules in sickle cell disease: effect of hydroxyurea. *Transfus Clin Biol.* 2008;15(1-2):39-50.
28. El Nemer W, Gane P, Colin Y, et al. The Lutheran blood group glycoproteins, the erythroid receptors for laminin, are adhesion molecules. *J Biol Chem.* 1998;273(27):16686-16693.
29. Berk DA, Hochmuth RM. Lateral mobility of integral proteins in red blood cell tethers. *Biophys J.* 1992;61(1):9-18.
30. Beutler E. Gaucher disease. *Blood Rev.* 1988; 2(1):59-70.
31. Stoltz JF, Lucius M. Viscoelasticity and thixotropy of human blood. *Biorheology.* 1981;18(3-6):453-473.
32. Baskurt OK, Meiselman HJ. RBCs aggregation: more important than RBCs adhesion to endothelial cells as a determinant of in vivo blood flow in health and disease. *Microcirculation.* 2008;15(7): 585-590.
33. Frenette PS. Sickle cell vasoocclusion: heterotypic, multicellular aggregations driven by leukocyte adhesion. *Microcirculation.* 2004;11(2):167-177.
34. Kato GJ, Hebbel RP, Steinberg MH, Gladwin MT. Vasculopathy in sickle cell disease: Biology, pathophysiology, genetics, translational medicine, and new research directions. *Am J Hematol.* 2009;84(9):618-625.
35. Nash GB, Johnson CS, Meiselman HJ. Rheologic impairment of sickle RBCs induced by repetitive cycles of deoxygenation-reoxygenation. *Blood.* 1988;72(2):539-545.
36. Barabino GA, Platt MO, Kaul DK. Sickle cell biomechanics. *Annu Rev Biomed Eng.* 2010;12:345-367.
37. Kaul DK, Fabry ME. In vivo studies of sickle red blood cells. *Microcirculation.* 2004;11(2):153-165.
38. Almeida A, Roberts I. Bone involvement in sickle cell disease. *Br J Haematol.* 2005;129(4):482-490.
39. El Nemer W, Wautier MP, Rahuel C, et al. Endothelial Lu/BCAM glycoproteins are novel ligands for red blood cell alpha4beta1 integrin: role in adhesion of sickle red blood cells to endothelial cells. *Blood.* 2007;109(8):3544-3551.
40. Gauthier E, Rahuel C, Wautier MP, et al. Protein kinase A-dependent phosphorylation of Lutheran/basal cell adhesion molecule glycoprotein regulates cell adhesion to laminin alpha5. *J Biol Chem.* 2005;280(34):30055-30062.
41. Inokuchi J, Momosaki K, Shimeno H, Nagamatsu A, Radin NS. Effects of D-threo-PDMP, an inhibitor of glucosylceramide synthetase, on expression of cell surface glycolipid antigen and binding to adhesive proteins by B16 melanoma cells. *J Cell Physiol.* 1989;141(3):573-583.
42. Groener JE, Poorthuis BJ, Kuiper S, Hollak CE, Aerts JM. Plasma glucosylceramide and ceramide in type 1 Gaucher disease patients: correlations with disease severity and response to therapeutic intervention. *Biochim Biophys Acta.* 2008;1781(1-2):72-78.
43. Meikle PJ, Whitfield PD, Rozaklis T, et al. Plasma lipids are altered in Gaucher disease: biochemical markers to evaluate therapeutic intervention. *Blood Cells Mol Dis.* 2008;40(3):420-427.
44. Boven LA, van Meurs M, Boot RG, et al. Gaucher cells demonstrate a distinct macrophage phenotype and resemble alternatively activated macrophages. *Am J Clin Pathol.* 2004;122(3):359-369.
45. Moran MT, Schofield JP, Hayman AR, Shi GP, Young E, Cox TM. Pathologic gene expression in Gaucher disease: up-regulation of cysteine proteinases including osteoclastic cathepsin K. *Blood.* 2000;96(5):1969-1978.